Complex Conductivity of YBCO Films in Normal and Superconducting States Probed by Microwave Measurements

J. Krupka, J. Wosik, C. Jastrzębski, T. Ciuk, J. Mazierska, and M. Zdrojek

***Abstract*—We report on microwave frequency characterization of yttrium barium copper oxide (YBCO) thin films in both normal and superconducting states. A microwave single-post dielectric resonator technique using two different resonators was used for the complex conductivity determination of YBCO samples deposited on dielectric substrates. The intrinsic complex conductivity of YBCO films was determined from the measured resonator quality factor Q and resonant frequency values employing rigorous electromagnetic modeling of the resonant structures with the mode-matching and Rayleigh–Ritz techniques. Such approach allowed us to determine the intrinsic properties of the films (conductivity, permittivity, and penetration depth) without any simplifications and errors associated with approximate modeling employing perturbation theory. We describe the superconducting material only through its intrinsic material properties, such as the complex conductivity, which does not depend on the thickness of the sample and other parameters. From both simulations and experimental results, we show that the proposed method of intrinsic complex conductivity determination is particularly useful for the characterization of very thin YBCO layers. To support the novelty of our approach, it is shown that significant differences appear between the rigorous and perturbation computations for thin superconducting films (below 50 nm).**

***Index Terms*—Microwave conductivity, superconductors, two-fluid model, yttrium barium copper oxide (YBCO).**

I. Introduction

FORMALLY, at microwave frequencies, the intrinsic electromagnetic properties of superconductors can be characterized by the complex conductivity or by the complex permittivity tensors. At microwave frequencies, the real part of the complex permittivity of a superconductor is negative and describes the so-called kinetic inductance, while the imaginary part describes the losses. Superconductor in the normal state behaves like a normal conductor that can be characterized by normal conductivity.

Most methods intended for the characterization of the material properties of the superconductors at microwave frequencies employ resonance cavities and other resonators, since resonators exhibit high measurement sensitivity due to their large Q-factor values. The ideal resonator for this purpose should have parasitic losses that are small compared to losses in the sample. One of the most convenient resonators intended for measurements of the surface resistance of high-temperature superconductors (HTSs) in the superconducting state is a sapphire rod dielectric resonator with two end plates made of superconducting samples. Such resonators were introduced independently by a few research groups [1]–[3], and now, they are routinely used for the characterization of the HTSs by many research and industrial laboratories [4]. The sapphire rod resonator method is simple and has almost negligible parasitic losses due to the extremely low dielectric losses of sapphire.

A very useful technique for microwave characterization of superconducting materials having small sizes and complex structures, such as high-T_c superconductors, is a cavity-perturbation technique. A sapphire-hot finger combined with the TE_{011} resonators, made out of bulk niobium [5] or coated with PbSn alloy [6], is used in this technique. The superconducting sample is placed at an E-field node, which is an H-field antinode, and on an independently temperature-controlled sapphire rod, whereas the superconducting resonator is kept at liquid helium temperature. Such a configuration allows one to differentiate the temperature-dependent HTS sample response from the superconducting resonator background. This technique allows precise determination of the surface resistance as well as the determination of the penetration depth for HTS single crystals and thin-film samples. It can also be used for anisotropy measurements due to the polarization of the microwave field in the sample location. A similar approach, with better filling factors, was also reported when split or gap loop resonators were employed [7].

Another resonator that has been frequently used for measurements of the sheet impedance of thin superconducting films is the TE_{011} mode cavity terminated at one bottom by a superconducting sample [8]–[10].

Usually, there are two parameters reported for HTSs at microwave frequencies, namely, the wave resistance and the penetration depth, or wave impedance. The wave impedance which is defined for bulk material describes the surface

Manuscript received September 24, 2012; revised November 13, 2012 and December 10, 2012; accepted December 13, 2012. Date of current version January 30, 2013. This work was supported in part by Project N R02 004210. This paper was recommended by Associate Editor B. Plourde.

J. Krupka and T. Ciuk are with the Institute of Microelectronics and Optoelectronics, Warsaw University of Technology, 00-662 Warsaw, Poland (e-mail: krupka@imio.pw.edu.pl).

J. Wosik is with the Electrical and Computer Engineering Department and Texas Center for Superconductivity, University of Houston, Houston, TX 77204 USA.

C. Jastrzębski and M. Zdrojek are with the Faculty of Physics, Warsaw University of Technology, 00-662 Warsaw, Poland.

J. Mazierska is with the School of Engineering and Physical Sciences, James Cook University, Townsville, QLD 4811, Australia.

Color versions of one or more of the figures in this paper are available online at http://ieeexplore.ieee.org.

Digital Object Identifier 10.1109/TASC.2012.2237515

resistance of a superconducting film deposited on a dielectric substrate very well when the film thickness is two to three times larger than the penetration depth. Determination of the electrical parameters of superconductors at temperatures around the critical temperature is not as simple as it is for temperatures well below T_c. At higher temperatures, the superconducting film thickness (typically a few hundred nanometers) becomes comparable (or smaller) to the penetration or normal-state skin depth. In such a case, electromagnetic fields penetrate partly through the film, and the sample cannot be treated as a bulk case. As a consequence, the surface impedance of the sample is no longer defined just in terms of the intrinsic properties of the superconductor but also depends on other parameters, including thickness and substrate permittivity. In addition, the Q-factors of sapphire resonators terminated by thin superconducting films in the normal state, deposited on dielectric substrates, are too suppressed to be measurable. Therefore, for such measurements, another types of resonators are preferable, including, for example, copper TE_{011} mode cavities. All these problems become more pronounced when the thickness of the film is small and the permittivity of the substrate is large and, in addition, exhibits strong temperature dependence as, e.g., for $SrTiO_3$ substrate [8].

The typical approach for the determination of the wave impedance of the superconductors is perturbation theory. Properly used extended perturbation theory [8], [10] (with the impedance transformation) allows the determination of the wave impedance of a superconductor with similar precision that would be achieved with rigorous electromagnetic approach particularly for superconducting films of a typical thickness (a few hundreds of nanometers). As it will be shown in this paper, more significant differences between rigorous and perturbation approaches may appear when film thickness becomes very thin (below 50 nm) and at temperatures that are close or higher than the critical temperature of a superconductor.

The first objective of this paper is to use such approach to determine the intrinsic complex conductivity (or the complex permittivity) of thin superconducting films at a broad temperature range from 4 K to 300 K and at few frequencies, employing identical relatively small samples deposited on typical 10 mm $\times$ 10 mm substrates. The second objective is to provide the complex permittivity and the complex conductivity measurements for yttrium barium copper oxide (YBCO) films.

II. Theory

Here, we briefly describe the electromagnetic properties of the thin superconducting films at microwave frequencies. The two-fluid conductivity model [11], [12] is generally accepted for the formal description of the electromagnetic properties of superconductors. According to this theory, the conductivity of a superconductor at temperatures lower than the critical temperature of a superconductor T_c is a complex quantity $\sigma(\omega) = \sigma_1(\omega) - j\sigma_2(\omega)$ (where σ_1 is responsible for loss, and σ_2 is responsible for the kinetic inductance). At temperatures higher than the critical temperature, the imaginary part of the conductivity is equal to zero, and the real part fully describes its electric properties.

Measurement and modeling of superconductors at microwave frequencies require accurate knowledge of their material properties. To determine measurable quantities for a specific device, such as a resonant cavity containing a superconducting sample, it is necessary to solve Maxwell's equations assuming that all cavity parameters (material properties and dimensions) are known. Electromagnetic properties of a physical medium in Maxwell's equations for time harmonic electromagnetic fields are characterized by the complex permittivity and the complex permeability. Conductivity of the medium, if present, is included in the imaginary part of the complex permittivity according to the following formulas:

$$\varepsilon = \varepsilon_0 \left(\varepsilon_{1p} - j\varepsilon_{2p} - j\frac{\sigma}{\omega\varepsilon_0} \right) \tag{1}$$

where ε_0 is the permittivity of the vacuum, ε_{1p} and ε_{2p} are the real and imaginary parts of the permittivity due to dielectric polarization mechanisms, ω is the angular frequency, and σ is the conductivity.

Substituting the complex conductivity into (1) and neglecting ε_{1p} and ε_{2p}, one obtains the following expression for the complex permittivity of a superconductor:

$$\varepsilon = \varepsilon_0 \left(-\frac{\sigma_2}{\omega\varepsilon_0} - j\frac{\sigma_1}{\omega\varepsilon_0} \right). \tag{2}$$

One can notice that, at microwave frequencies, the real part of the complex permittivity of a superconductor in its superconducting state is negative. Additional quantities that are defined for a bulk medium, to characterize its interaction with electromagnetic fields, are the intrinsic wave impedance $Z = (\mu/\varepsilon)^{0.5}$ and the complex propagation constant $\gamma = \alpha + j\beta$, where $\gamma^2 = -\omega^2\varepsilon\mu$. For a nonmagnetic superconductor ($\mu = \mu_0$), its intrinsic wave impedance and propagation constant can be expressed as $Z_S = (-\omega\mu_0/\sigma_2 + j\sigma_1)^{0.5}$ and $\gamma^2 = \omega\mu_0(\sigma_2 + j\sigma_1)$, respectively. This shows that, for a perfect superconductor, where $\sigma_1 = 0$, the wave impedance is purely imaginary, while for substances with $\sigma_2 = 0$ (metals, including superconductors in the normal state), it is a complex quantity with equal real and imaginary parts. Electromagnetic fields in superconductors in both the superconducting and the normal state decay exponentially. The length over which the electromagnetic field decays by a factor of e is called the penetration depth λ. It can be evaluated as $\lambda = 1/\alpha$, and it generally depends on the two complex conductivity components. For a perfect superconductor with $\sigma_1 = 0$, the penetration depth is equal to the London penetration depth $\lambda_L = (1/\omega\mu_0\sigma_2)^{0.5}$. It should be noted that a perfect superconductor does not dissipate electromagnetic energy, and the electromagnetic fields decay exponentially along the direction which is normal to its surface. For superconductors in the normal state, as for all other normal conductors, the depth at which the electromagnetic fields decay to $1/e$ is called the skin depth δ and can be determined as $\delta = (2/\omega\mu_0\sigma_1)^{0.5}$. As it will be shown later, at microwave frequencies, for YBCO films of thicknesses in the range 30–600 nm, the penetration depth will frequently be larger than the film thickness. In such a case, films become semitransparent to the electromagnetic field, and as the result, the surface

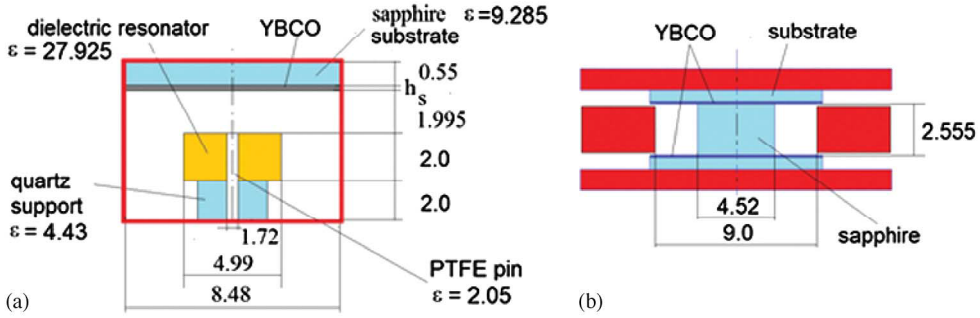

Fig. 1. Sketch of the experimental setup. (a) $TE_{0n\delta}$ mode 13.3-GHz single-post dielectric resonator made of BZT ceramic with permittivity equal to 27.93 at 300 K. (b) Sapphire rod resonator operating at 28.2 GHz (TE_{011} mode) and 44.40 GHz (TE_{021} mode) at 13 K. All dimensions in the resonators are marked in millimeters.

resistance and the surface reactance will depend not only on the complex conductivity of the film but also on other parameters such as the film and substrate thicknesses, the substrate permittivity, and the electric properties of metal surfaces behind the substrate.

III. Experiments

Two different configurations of dielectric resonators were used in our experiments. The first—the single-post dielectric resonator—was designed to measure the conductivity of the very thin semitransparent and lossy films. Its construction was similar to that used for measurements of the sheet resistance of graphene [13]. The dielectric resonator was made from low-loss high-permittivity barium zirconium titanate (BZT) ceramic. With this resonator, we have performed the temperature-dependent measurements of the conductivity σ_1 of YBCO in the normal state and the conductivities σ_1 and σ_2 in the phase transition from the normal to the superconducting state. The second configuration—the sapphire rod resonator—was used for measurements of the conductivities σ_1 and σ_2 in the superconducting state. Sketches of our resonators showing their configurations and dimensions are presented in Fig. 1. It should be noted that, in experimental setups, square YBCO samples extend well beyond the copper cavity enclosures for both configurations. Resonators were mounted on a cold finger of our closed-cycle two-stage helium cryostat.

In our modeling, regions outside the diameter of the cavity enclosures have been neglected because the electromagnetic fields there have evanescent character. It should be noted that both resonators that are shown in Fig. 1 have similar inner diameters of the metal cavities and that the thickness of the gap where our rectangular samples are inserted is only about 0.5 mm. The gap size is therefore much smaller than the half of wavelength corresponding to the resonance frequencies for both resonators. As the result, the electromagnetic fields in the substrates decay rapidly in radial direction outside the diameter of the metal cavities. Similar simplifications have been used in the past with sapphire rod and single-post dielectric resonator techniques. They are well justified, and they reduce electromagnetic modeling to axially symmetric structures.

Experiments have been carried out with two types of YBCO thin films, which were obtained from THEVA. The films were deposited on sapphire substrates having dimensions of 10 mm $\times$ 10 mm $\times$ 0.55 mm. The substrates were initially covered with CeO_2 buffer layers of 40-nm thickness, and then, YBCO films of thicknesses of 30 and 280 nm, respectively, were deposited on them. For the 30-nm extra-smooth-type films, the critical temperature and the critical current density specified by the manufacturer were 83.5 K and 0.9 MA/cm^2, respectively. The critical temperature of 280-nm films was nominally equal to 86 K. Measurements of the resonance frequencies and Q-factors have been performed employing a microwave network analyzer (Agilent Technologies four-port PNA model operating up to 50 GHz) which displays information on the loaded Q-factor Q_L of resonators in transmission mode using multipoint fit on the complex values of S_{21} (transmission coefficient). Our resonators were equipped with precise coupling mechanisms based on coupling loops terminated with 1.1-mm-diameter semirigid coaxial cables. They allowed us to adjust couplings on both two resonator ports to such weak values that their influence on the unloaded Q-factor Q_L is only on the order of 1%. It requires both ports to have equal couplings and transmission coefficient $|S_{21}| < -40$ dB at the resonance frequency. In addition, the influence of coupling was accounted for, employing a well-known relation between the loaded and the unloaded Q-factor values for equal couplings: $Q_u = Q_L/(1 - |S_{21}|)$.

The results of the measurements of the $TE_{01\delta}$ mode resonance frequency shifts and Q-factors versus temperature for our 13.3-GHz single-post dielectric resonator containing 30- and 280-nm YBCO films are shown in Fig. 2. Changes of the resonance frequency $f(T) - f(T = 13\ \mathrm{K})$ were determined with respect to the resonance frequency $f(T = 13\ \mathrm{K})$ of the resonator containing a bulk copper sample kept at 13 K (the lowest temperature available in the cryostat containing the resonator). Fig. 2(a) shows that the resonance-frequency–temperature drifts of the resonator containing the blank substrate and the resonator containing the bulk copper sample have identical shapes and differ by about 39 MHz. For the 280-nm-thick YBCO film, the resonance frequency shifts versus temperature are only slightly different than that for the bulk copper sample. For the YBCO film of 30-nm thickness, the resonance frequency shifts are similar to that for bulk copper only at temperatures below 80 K (at the superconducting state of the film). At temperatures above 80 K, the resonance frequency shifts for 30-nm-thick sample become large. This is because the 30-mm sample in the normal state is semitransparent

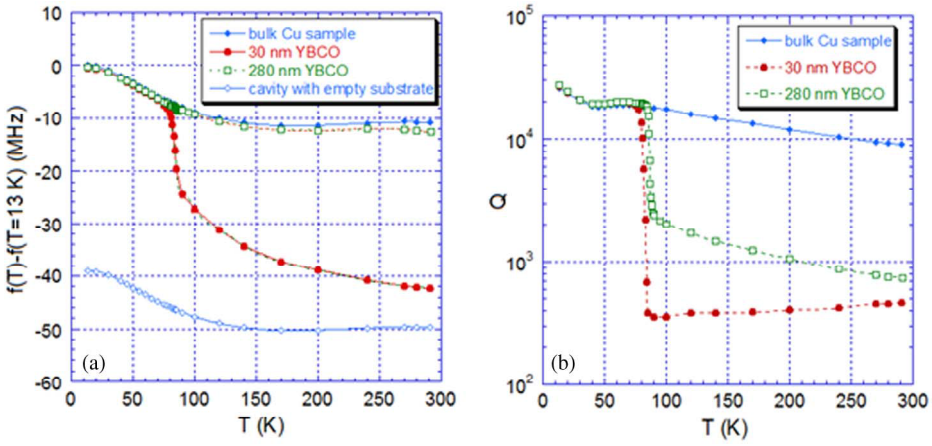

Fig. 2. (a) Plot of the $TE_{01\delta}$ mode resonance frequency shifts and (b) Q-factors as a function of temperature performed in the 13.3-GHz single-post dielectric resonator containing single YBCO films having thicknesses of 30 and 280 nm, respectively, and deposited on 0.55-mm sapphire substrates.

to the electromagnetic fields. It should be noted that the resonance frequency shifts due to the presence of the superconducting sample $f - f_{\rm ref}$ can be determined by subtracting the resonance frequency shifts $f(T) - f(T = 13\ {\rm K})$ for the bulk copper sample from the shifts for superconducting samples. The Q-factors due to the presence of the superconducting film $(Q_{\rm YBCO})$ were obtained from the following equation:

$$Q_{\rm YBCO}^{-1} = Q_{\rm sup}^{-1} - Q_{\rm parasitic}^{-1} \tag{3}$$

where $Q_{\rm sup}$ is the measured unloaded Q-factor of the resonator containing the sample under test, whereas $Q_{\rm parasitic}$ and $Q_{\rm YBCO}$ are the Q-factors due to the parasitic and bare sample losses, respectively.

The Q-factor due to the parasitic losses depends on all losses in the resonator except the losses in the sample and can be determined on the basis of measurements of the Q-factor of the resonator with bulk copper sample Q_m from

$$Q_{\rm parasitic}^{-1} = Q_m^{-1} - Q_{\rm COPPER}^{-1} \tag{4}$$

where Q_m is the measured unloaded Q-factor of the resonator containing copper reference sample and $Q_{\rm COPPER}$ is the Q-factor due to the losses in the reference copper sample only

$$Q_{\rm COPPER} = G_S / R_{S\rm Cu}. \tag{5}$$

The value for $Q_{\rm COPPER}$ was determined from independent measurements of the surface resistance of bulk copper $R_{S\rm Cu}$ with the sapphire rod resonator knowing the computed value of the geometric factor G_S for the sample in our resonator. It should be mentioned that the surface resistance value $R_{S\rm Cu}$ must be appropriately scaled to the frequency of our resonator and that the geometric factor is determined with a Rayleigh–Ritz technique from

$$G_S = \frac{\omega \iiint_V \mu_0 \mathbf{H} \cdot \mathbf{H}^* dv}{\iint_S \mathbf{H_t} \cdot \mathbf{H_t^*} ds} \tag{6}$$

where $\mathbf{H}$ is the magnetic field vector in the resonator containing a perfectly conducting sample, V is the volume of the resonator, S is the surface of the sample, and * is the complex conjugate symbol.

The volume integral in the numerator of (6) extends over the whole volume of the resonator, and the surface integral in the denominator extends only over the surface of YBCO sample(s). Thus, from the measurements of the resonance frequencies and Q-factors of the single-post dielectric resonator containing the sample under test, and the reference (copper) sample, it is possible to determine the resonance frequency shifts and Q-factors due to the presence of the test sample.

For the measurement with the sapphire rod resonator, Q-factors depend predominantly on the losses in the test samples because parasitic losses are almost negligible for the sapphire resonator inserted in a sufficiently large diameter cavity enclosure. The resonance frequency shifts for the sapphire resonator are determined as the difference between the resonance frequencies measured with the superconducting sample and the resonance frequency measured with a reference bulk copper sample. The resonance frequency and Q-factor changes of the sapphire rod resonator due to the complex conductivity of test sample(s) are much larger than those of the single-post dielectric resonator. Therefore, the sapphire rod resonator allows precise measurements of the Q-factors, which depend on the losses in the samples in the superconducting state. However, this technique has some drawbacks. First, in order to maintain its high Q-factor and high measurement sensitivity, the sapphire rod resonator requires two identical test samples. Second, due to the rapid changes of the Q-factor with increasing losses in the samples, it is impossible to measure samples in the normal state. This is due to the Q-factor degradation of the resonator with such samples to below measurable values. Third, disassembly is required to replace the samples; therefore, measurements of the resonance frequency shifts with the sapphire rod resonator are more difficult (and less accurate) than those with the single-post dielectric resonator. For the reasons discussed previously, measurements with the sapphire rod resonator were only possible at temperatures lower than the critical temperature of YBCO films. The results of measurements of the resonance frequency shifts and Q-factors due to losses in the superconducting samples employing the TE_{011} and TE_{021} modes excited in the sapphire rod resonator are shown in Fig. 3.

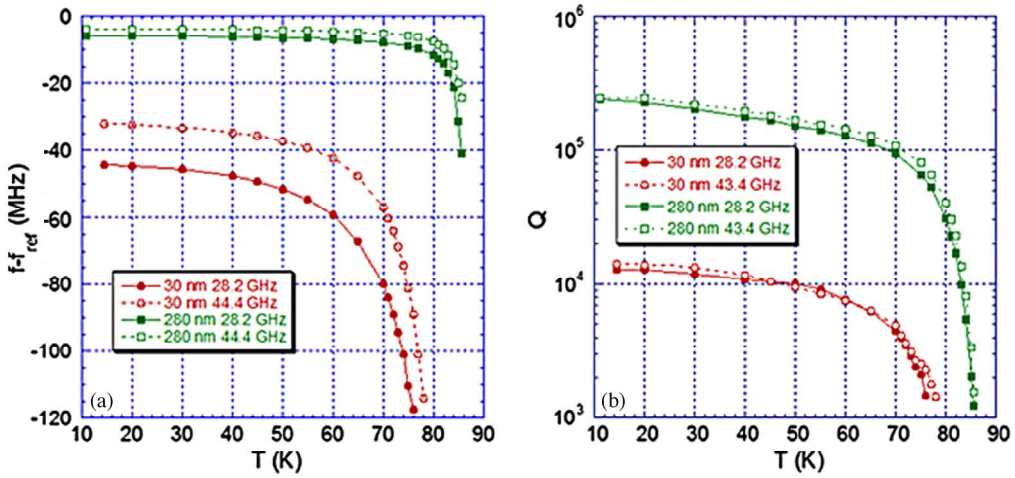

Fig. 3. Plots of (a) resonance frequency shifts and (b) Q-factors as a function of temperature for 30- and 280-nm YBCO films measured in sapphire rod resonator operating on the TE_{011} and TE_{021} modes.

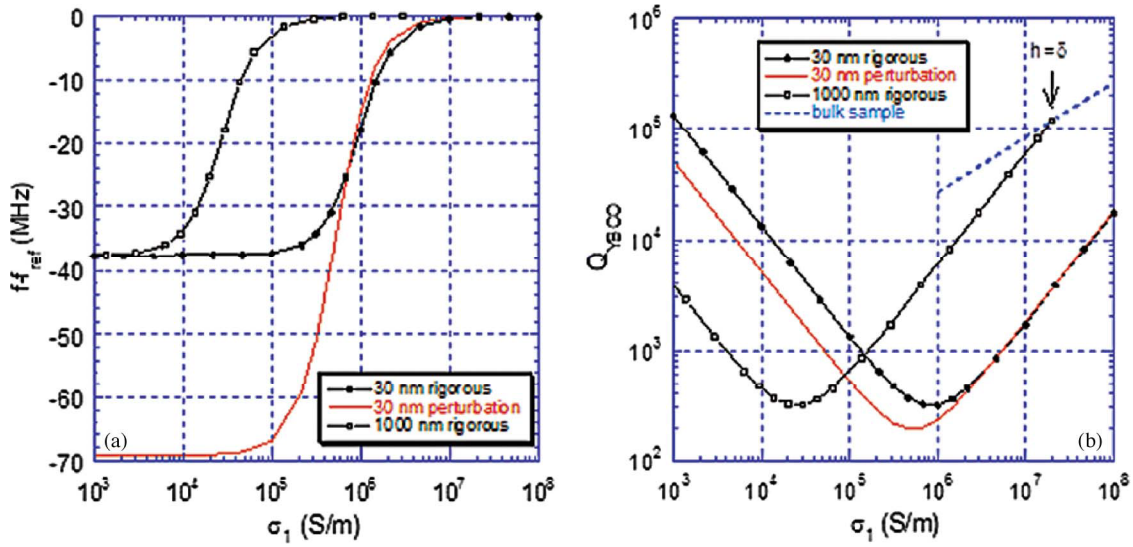

Fig. 4. (a) Calculated $TE_{01\delta}$ mode resonance frequency shifts and (b) Q-factor due to conductor losses versus conductivity for two sample thicknesses (30 and 1000 nm) for 13.3-GHz single-post dielectric resonator.

In order to evaluate the complex conductivity of the samples, we performed a rigorous electromagnetic modeling of our resonance structures employing the mode-matching and Rayleigh–Ritz techniques and the complex resonance frequency formalism [14], [15]. Alternatively, any commercial microwave simulators like HFSS, QuickWave, or Microwave Studio can be used for this purpose. Analyses have been performed assuming that all parts of the resonator (e.g., metal enclosure and dielectrics), but not the superconductor film, are lossless.

Now, we discuss the methodology of the conductivity determination for YBCO films in the normal state from the measurement data shown in Fig. 2. The results of the computations of the resonance frequency shifts and Q-factors due to conductor losses in the sample for our single-post dielectric resonator are shown in Fig. 4. It is important to distinguish between the resonator behavior for the case of thin samples having thickness smaller than the skin depth and for bulk samples having thickness a few times larger than the skin depth. For thin samples, the Q-factor slope above the minimum is equal to unity and depends on the product of conductivity and film thickness, while for bulk samples, the slope is equal to 0.5 and depends on the conductivity but not on the film thickness. Curves for thin samples and for bulk samples cross over at the conductivity value for which the skin depth is approximately equal to the film thickness. More information about such behavior and about the method of conductivity determination can be found in [13] and [16]. Apart from rigorous solutions, we have also shown in Fig. 4(a) and (b) the results of the computations of resonance frequency shifts and Q-factors for 30-nm sample employing the extended perturbation theory which assumes impedance transformation approach for the layer structure of the YBCO film and the constant value of rigorously computed geometric factor for a well-conducting sample. One can conclude that the results of the perturbation theory for 30 nm agree very well with rigorous results for conductivity values that are larger than 2×10^6 S/m. For small conductivity values, the slopes and shapes of the curves obtained with rigorous calculations and

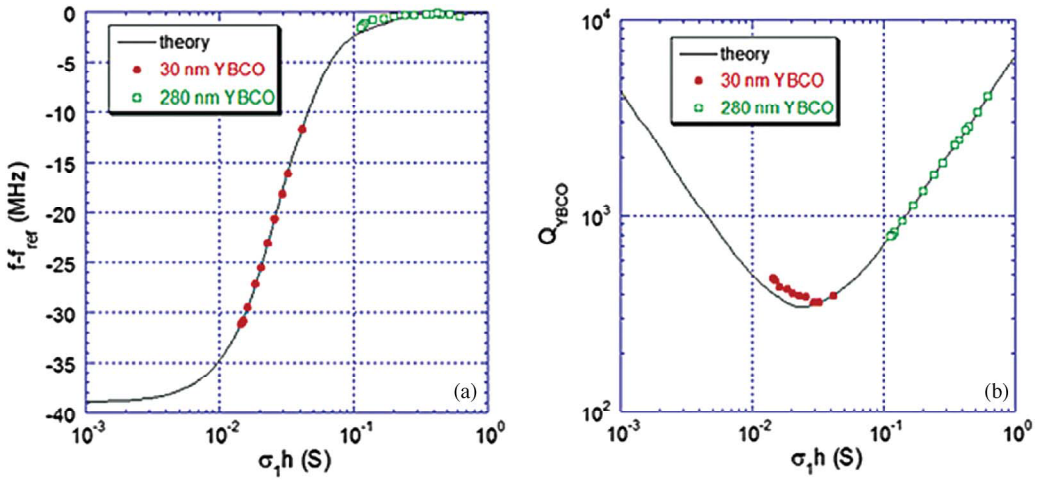

Fig. 5. (Points) Experimental data on the background of theoretical resonance frequency shifts and (lines) Q-factor due to conductor losses for 13.3-GHz single-post dielectric resonator. (a) Resonance frequency shifts. (b) Q-factor due to losses in YBCO films.

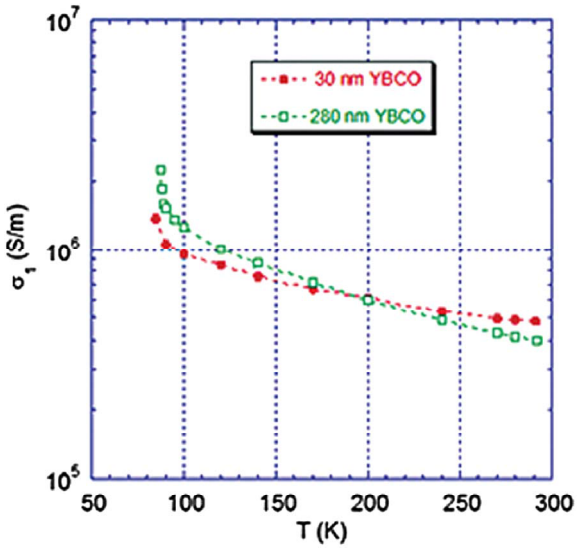

Fig. 6. Extracted normal conductivity σ_1 for 30- and 280-nm YBCO films as a function of temperature.

perturbation theory agree, but there are qualitative differences in both resonance frequency shifts and Q-factor the order of 50%. For thicker samples, the range of conductivities where the two theories match is extended toward lower conductivity values, which indicates that, for such samples, perturbation and rigorous approaches can alternatively be used.

Experimental values of the resonance frequency shifts and Q-factors due to the losses in the sample are presented in Fig. 5 along with theoretical curves for our 30- and 280-nm samples, and Fig. 6 shows the extracted conductivity values of these samples. To show this, we used a reconstruction algorithm for the conductivity determination. In the conductivity range where the slope of the resonance frequency shift is steep and the Q-factor value approaches minimum, we have determined the conductivity from the frequency shift values; otherwise, we have determined the conductivity from the Q-factor values. Due to unavoidable experimental errors, the overdetermined system of two nonlinear equations with respect to the one unknown (conductivity) will not be perfectly satisfied, which leads to the discrepancy between experimental data and that theoretical curve that was not used in the conductivity determination. There are two possible solutions to get a better fit between experimental and theoretical results. In the first approach, one can solve the system of two nonlinear equations with respect to conductivity in the sense of minimum least square error, but the problem is how to choose the weight coefficients on two different measured quantities (resonance frequency shifts and Q-factors). The other way is to introduce an additional parameter, e.g., thickness of the substrate, as the second unknown and solve the system of two nonlinear equations with respect to two unknowns but at the cost of substantial numerical effort.

Based on the results that are shown in Fig. 6, one can conclude that the conductivities of 30- and 280-nm films are comparable and exhibit similar slopes versus temperature, although the Q-factor slopes versus temperature for these samples have different signs [as can be seen in Fig. 2(b)]. Both the 30- and 280-nm samples have a thickness much smaller than the skin depth. The extended perturbation theory (with impedance transformation) gives conductivity results that are almost identical to those which were obtained with the rigorous method for 280-nm sample, but for 30-nm sample, the perturbation theory gives Q-factor values below experimental data points, as can be seen in Fig. 4. See the comparison of rigorous and perturbation techniques in the supplementary information.

Determinations of both the real and imaginary parts of the conductivity in the superconducting state are more complicated than the conductivity in the normal state. This is because, generally, both the resonance frequency shifts and the Q-factors due to the losses in YBCO samples depend in a complicated manner on both the real and the imaginary part of the complex conductivity as well as on the thickness of the samples. In order to determine both conductivity components, we first computed the resonance frequency shifts for fixed resonator geometry and the number of expected values of σ_1 and σ_2, creating "lookup tables." Then, we used the nonlinear equation solver (fsolve) in MATLAB to find the complex conductivity values for each experimental data point. To obtain the goal function

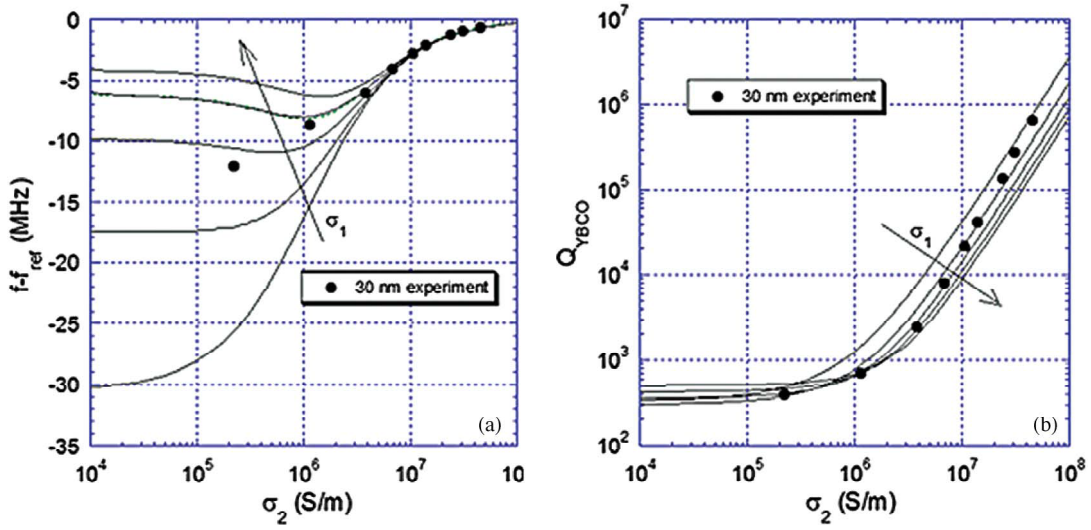

Fig. 7. Experimental data on the background of (a) theoretical resonance frequency shifts and (b) Q-factors due to losses in YBCO sample for 13.3-GHz single-post dielectric resonator and sample having a thickness of 30 nm. Particular lines correspond to the values of $\sigma_1 = [0.5, 1.0, 1.5, 2.0, 2.5] \times 10^6$ S/m.

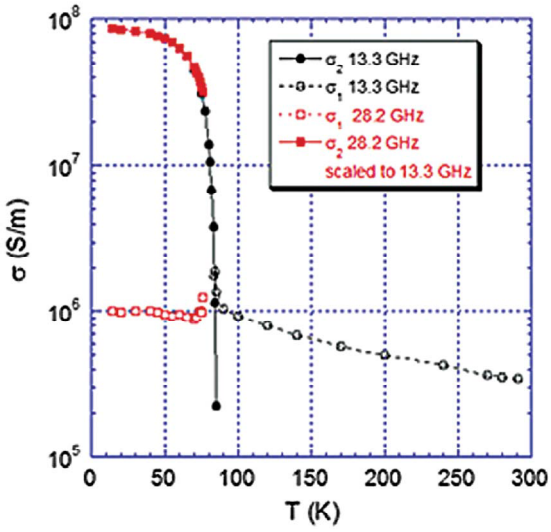

Fig. 8. Extracted conductivity components in transition from the normal state to the superconducting state for YBCO film of 30-nm thickness as a function of temperature measured at 13.3 GHz. The red data points marked with squares are scaled from sapphire rod dielectric resonator measurement performed at 28.2 GHz.

of continuous variables σ_1 and σ_2, a cubic spline interpolation was used on the lookup table data. In Fig. 7, experimental values of the resonance frequency shifts and Q-factors due to losses in the sample are presented along with theoretical curves for the 30-nm sample measured in the 13.3-GHz single-post dielectric resonator. The results of the complex conductivity determination in broad temperature range are shown in Fig. 8.

It should be mentioned that, by employing 13.3-GHz single-post dielectric resonator, it would be theoretically possible to perform measurement close to the absolute value of the complex conductivity (and London penetration depth) at low temperature range on a hypothetical single-layer YBCO film because, for such sample, the resonance frequency shift values would be relatively large (a few megahertz) even at liquid helium temperatures, as it can be concluded from the theoretical prediction that is shown in Fig. 9(a). The London penetration depth value of 300 nm corresponds to the imaginary part of conductivity value of about 10^8 S/m, so for such a case, the resonance frequency shift would be equal to -7.5 MHz.

A similar measurement procedure was applied to determine the real and imaginary parts of the conductivity in the superconducting state from measurement data obtained with the sapphire rod resonator. In Fig. 10, experimental data are shown along with the theoretical resonance frequency shift and Q-factor for the TE_{011} mode of our sapphire resonator operating at 28.2 GHz. The results of conductivity determination for 30- and 280-nm samples from the measurement data with the sapphire resonator at two frequencies (28.2 and 44.4 GHz) are presented in Fig. 11.

We should remark that the determination of the absolute values of the imaginary part of conductivity at low temperatures (below the critical temperature of the superconductor) is difficult, and it is subjected to experimental uncertainties. One reason for this is that the reference frequency value is measured on a flat reference copper sample. Although the influence of a finite conductivity of copper on the resonance frequency shift is relatively small, such influence was taken into account, but larger experimental errors are still present due to the finite flatness and roughness of copper and YBCO surfaces. As the result, the surfaces of copper and YBCO films in real experiment are situated effectively at slightly different positions in the resonator along its z-axis. There are also additional systematic errors associated with resonator assembling/disassembling process, which are the main sources of measurement uncertainties for the imaginary part of conductivity (or penetration depth) determination. Because the resonance frequency shifts for very thin samples are few times larger than for the thicker samples, the determination of the absolute value of the imaginary part of conductivity for thin samples is possible, and it is much more accurate than for the thicker samples. As it is seen in Fig. 3, the resonance frequency shifts for our 28.2-GHz sapphire resonator with two 30-nm samples in the superconducting state are in the range from -44 MHz at 13 K to -117 MHz at 76 K.

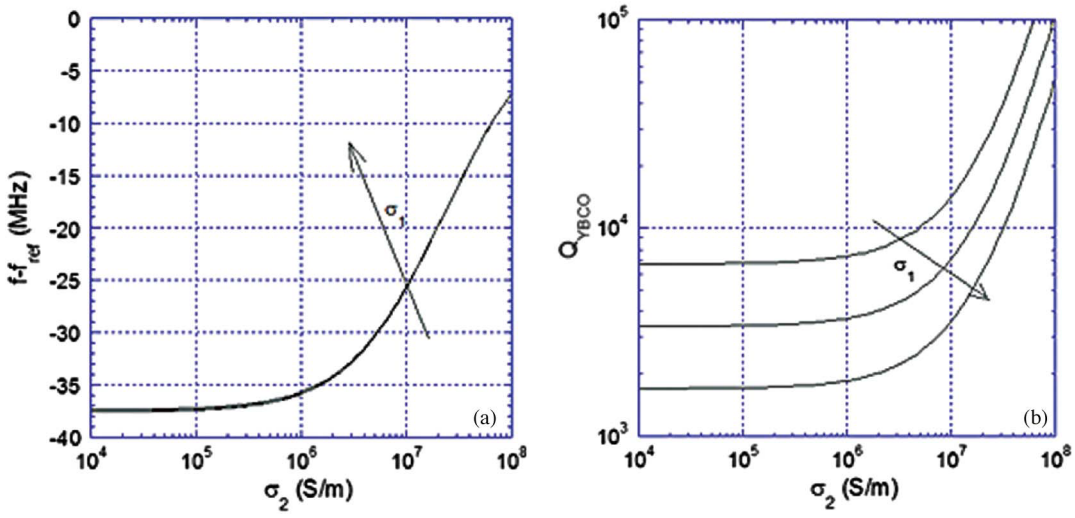

Fig. 9. (a) Theoretical resonance frequency shifts and (b) Q-factors due to losses in YBCO sample for 13.3-GHz single-post dielectric resonator and sample having a thickness of 1.18 nm (thickness of single-cell-layer YBCO). Particular lines correspond to the values of $\sigma_1 = [0.5, 1.0, 2.0] \times 10^6$ S/m.

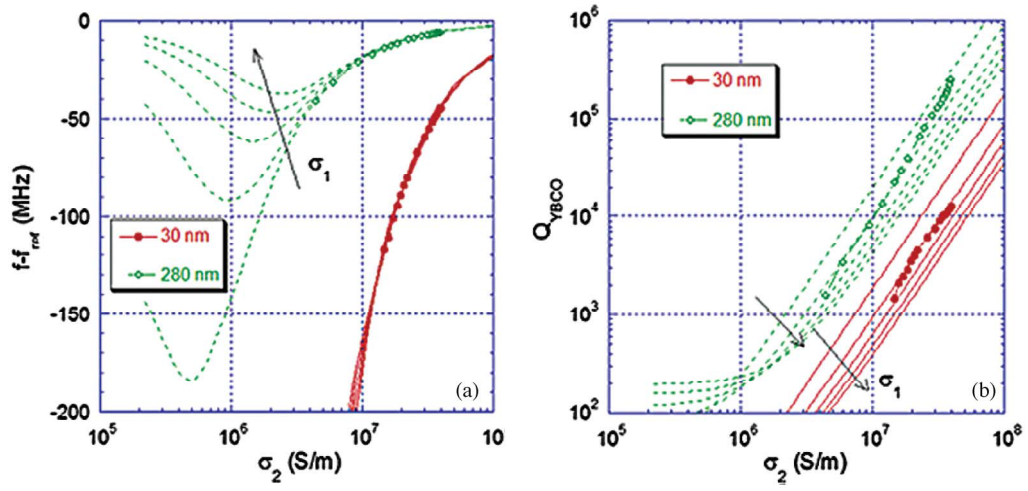

Fig. 10. Experimental data points measured at 28.2 GHz in sapphire resonator for two YBCO films are shown on the background of (a) the theoretical resonance frequency shift and (b) Q-factors plotted *versus* YBCO film losses. Discrete lines correspond to the values of σ_1 equal to $[0.5, 1.0, 1.5, 2.0, 2.5] \times 10^6$ S/m.

These values are few times larger than the variance of statistical errors of the resonance frequency measured after resonator assembling/disassembling. The value of the resonance frequency variance on five subsequent measurements of the 28.2-GHz resonance frequency resonator after its assembling/disassembling was about 5 MHz, and the theoretical value of the resonance frequency shift due to the finite conductivity of copper (related to the resonator with perfectly conducting surfaces) is about -0.8 MHz at 13 K. Thus, the total uncertainty of the resonance frequency shift is about eight times smaller than the resonance frequency shift value at 13 K (-44 MHz). This was one of the reasons for our experiments with 30-nm samples, so we can claim that measurements of the complex conductivity (and the London penetration depth) on 30-nm samples can be treated as the absolute ones, although with some degree of errors. The uncertainty of the absolute value of conductivity determination is additionally related to the uncertainties in the determination of the thickness of the sample. The London penetration depth value computed from σ_2 at 13 K for our 30-nm sample proved to be 330 nm. This result is about 80 nm larger than the value obtained by Klein *et al.* [10] on 160-nm sample deposited on $SrTiO_3$ substrate. Klein's value $\lambda_L(0) = 250$ nm given at 0 K limit was based on the empirical two-fluid model fit relation. For very thin samples, we can expect the degradation of their electromagnetic properties with respect to the samples of a medium thickness (200–300 nm), so the agreement between our result and Klein's result is quite good. Unfortunately, the resonance frequency shift value for the samples of 280-nm thickness at 13 K was only -6 MHz, which is within our measurement uncertainties, so the London penetration depth value for 280-nm-thick samples at 13 K cannot be treated as an absolute one. This is valid for any thicker samples. Therefore, we cannot exclude the possibility that the London penetration values for 30-nm samples are larger than those for 280-nm samples. On the other hand, the agreement between σ_2 values for 30- and 280-nm samples at 13 K is excellent, which is shown in Fig. 11.

In the case of measurement uncertainties of the complex conductivity employing resonance techniques, it should be pointed out that their main source is always related to the

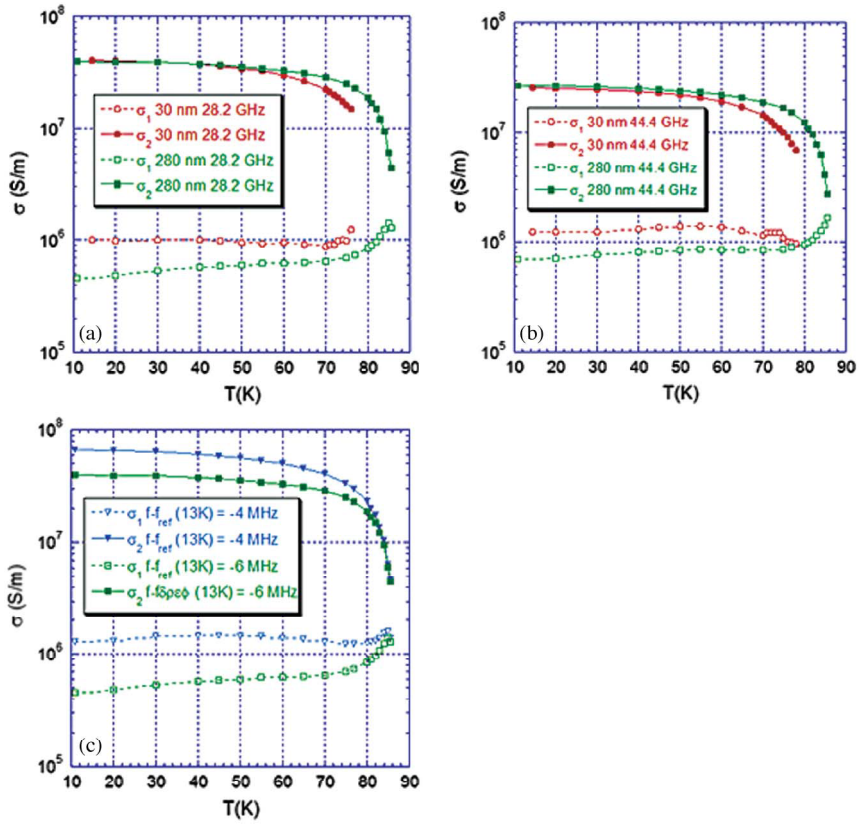

Fig. 11. Extracted conductivity components for two YBCO samples of thicknesses of 30 and 280 nm in superconducting state as a function of temperature. (a) and (b) depict the results at 28.2 and 44.4 GHz, respectively. (c) 280-nm sample at (green color) 28.2 GHz. The blue curves show the complex conductivity values evaluated for the reference frequency value shifted down by 2 MHz with respect to the original value.

determination of the initial resonance frequency shift between resonator containing superconducting sample(s) and resonator containing reference sample(s). To illustrate this, we have performed additional simulations (determination of the complex conductivity) assuming that the reference frequency value was shifted down by 2 MHz with respect to the measured value. The influence of such reference value change on the complex conductivity determination in 28.2-GHz sapphire resonator is shown in Fig. 11(c). As it is seen, changes of the reference frequency level have significant influence on the extracted conductivity values for 280-nm film. This is because the resonance frequency shift value for 280-nm sample at 13 K is small (-6 MHz). For 30-nm sample, the change of the reference frequency value by 2 MHz is not significant since the resonance frequency shift value at 13 K is about -44 MHz for this sample.

The following generally known conclusions can be drawn from our experimental results. The imaginary part of the conductivity varies with frequency as ω^{-1}. Such frequency dependence is confirmed with the measurement results at 13.3 GHz, where the frequency-scaled (from 28.2 to 13.3 GHz) imaginary part of the conductivity for the 30-nm film is also shown. The real part of the conductivity values is flat versus temperature for our samples, depending, to some extent, on the thickness of the sample and the measurement frequency, but their values are in the range from 0.5×10^6 to 1.2×10^6 S/m. Knowing the conductivity values, additional parameters such as the wave impedance for bulk samples and the penetration depth were evaluated employing (4) and (7). The results of the wave reactance, the wave resistance, and penetration depth computations are shown in Fig. 12. Wave reactance and wave resistance values were evaluated at 28.2 and at 44.4 GHz for the samples with 30- and 280-nm thicknesses. Note that the wave resistance scales with frequency proportionally to ω^2. The penetration depth in the superconducting state below the critical temperature practically does not depend on frequency, and at temperatures higher than the critical temperature, it converges to the frequency-dependent skin depth of a metal.

IV. Model

A. Theoretical Model of YBCO for Electromagnetic Simulators

The measurements results obtained on our samples, obtained from a leading manufacturer (THEVA), proved that, for the high-quality YBCO films, the real part of the conductivity σ_1 does not vary much as a function of temperature and frequency. Such regular behavior is probably related to the fact that, for the good-quality films, a normal conductivity component is predominantly related to nonpairing charge carriers [17]. Frequency and temperature dependences of the electrical properties of our YBCO films are therefore predominantly related to the temperature and frequency variations of the imaginary part of the conductivity. Let us assume for simplicity that σ_1 is constant and determine the wave reactance and the wave resistance for a hypothetical bulk YBCO sample as a

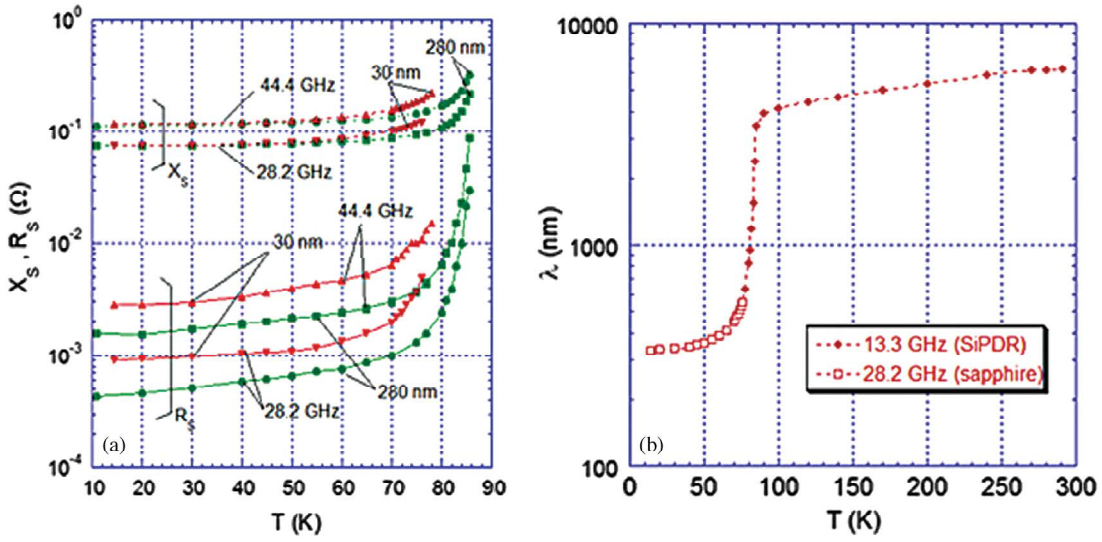

Fig. 12. (a) Wave impedance components versus temperature evaluated from conductivity values that are shown in Fig. 10. (b) Penetration depth as a function of temperature (for 30-nm sample).

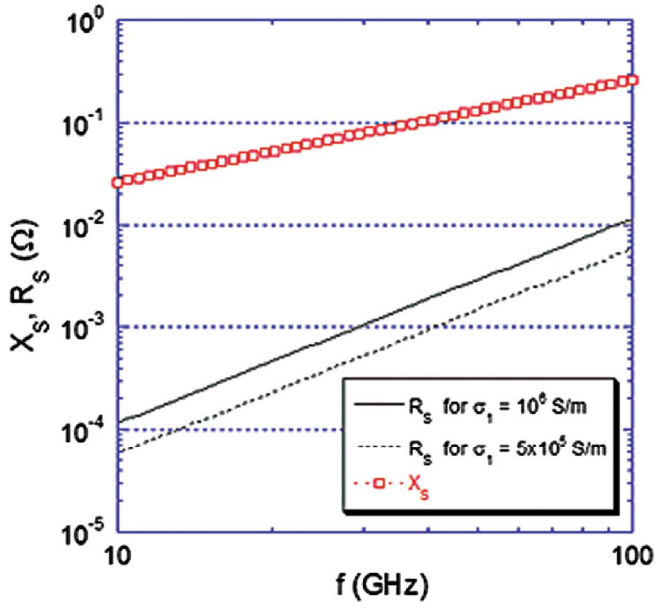

Fig. 13. Computed values of the wave reactance and the wave resistance as a function of frequency for two different normal conductivities are shown here. The wave reactance values are the same for both conductivities.

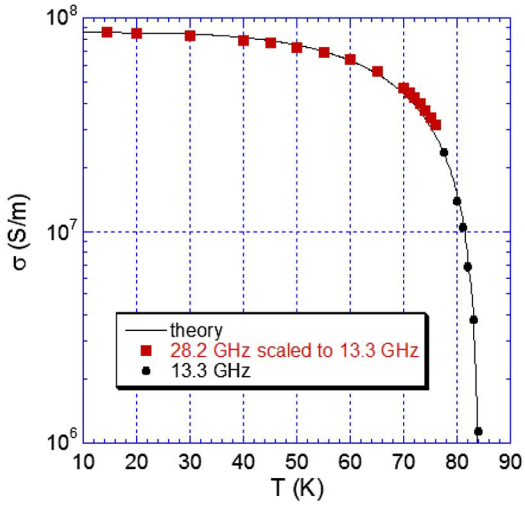

Fig. 14. Temperature dependence of the imaginary part of conductivity compared with the theoretical model at 13.3-GHz frequency for 30-nm sample.

function of frequency at a fixed temperature of 13 K. In our model, we assumed the imaginary part of the conductivity as 8.54×10^7 S/m at 13.3 GHz and its frequency dependence to be proportional to f^{-1}. This corresponds to the relative permittivity value of -1.154×10^8 at 13.3 GHz. The frequency dependence of the permittivity is proportional to f^{-2}. The results of the wave impedance determination for two different values of the real part of the conductivity are shown in Fig. 13. Computations have been performed for two values of the real part of the conductivity, namely, 5×10^5 and 10^6 S/m, because our experimental results mostly belong to this range. It is shown in Fig. 13 that, at 10 GHz, the real parts of the wave resistance values are 58 and 116 $\mu\Omega$, respectively, which are in a good agreement with the manufacturer's (THEVA) datasheet.

Let us now compare the temperature dependence of σ_2 that is shown in Fig. 8 with the theoretical model. In our model, we assume that $T_c = 84$ K and that the temperature dependence of σ_2 is

$$\sigma_2(T) = \sigma_2(0)\left[1 - \left(\frac{T}{T_c}\right)^4\right]. \tag{7}$$

The results of our modeling together with experimental data are shown in Fig. 14. It is seen that the agreement between theoretical model and experiment results is very good. This shows that the theoretical modeling of the microwave devices containing YBCO films of arbitrary thickness can be performed employing the two-fluid model. The advantage of such an approach is that, in commercial electromagnetic simulators, permittivity and conductivity are used as basic parameters for material description. Two constant quantities are sufficient for electromagnetic modeling in a broad frequency range, namely, the real part of the permittivity at a certain frequency (large

negative number) and the real part of the conductivity. If modeling is necessary as a function of temperature, then (7) can be used. It should be mentioned that the real part of the conductivity formally describes superconductor losses, regardless of their origin. These losses are the film quality dependent and may vary from one sample to another, depending on the manufacturing process.

V. Conclusion

A method that is based on rigorous solutions of Maxwell's equation has been proposed for the contactless measurements of the complex conductivity of the YBCO films. Such approach, which is typically used for accurate measurements of dielectrics and lossy ferroelectrics, allowed us to determine the intrinsic properties of the films without any simplifications and possible errors associated with the approximate modeling employing the perturbation theory. The complex conductivity of the YBCO films was determined from the measured resonator quality factor Q and resonant frequency values as a function of temperature. We have shown that, for thin films, our model significantly improves the accuracy of the complex permittivity determination when compared with the extended perturbation model. This is particularly for temperatures close to or higher than the critical temperature of a superconductor. It should be also noted that the proposed method is particularly useful for experimental studies of very thin superconducting films, because for such films, the measurement sensitivity is substantially enhanced with respect to the sensitivity for thicker films, thus allowing measurements of the absolute value of the imaginary part of conductivity (or London penetration depth).

Defining the electric properties of a superconductor by the frequency/temperature-dependent complex permittivity (with negative real part) allowed us to describe the superconductor in the same terms as any other material in electromagnetic modeling and to accurately specify the parameters of the model that can be conveniently used in electromagnetic simulators which are very important for microwave engineers. Very good agreement was achieved between the experimental data of complex conductivity and the values obtained from theoretical-based simulations. We should emphasize, however, that the properties of the YBCO films may vary from one manufacturer to another or even from one sample to another, so the complex permittivity/conductivity results that we obtained in this paper should not be treated as absolute values but rather as a good approximation of the parameters that characterize the high-quality YBCO films.

Acknowledgment

The authors would like to thank THEVA Duennschichttechnik GmbH for manufacturing the YBCO samples that were used in their experiments.

References

[1] O. Llopis, T. Parra, J. C. Ousset, D. B. Chrisey, J. S. Horwitz, and J. Graffeuill, "Comparative study of microwave surface impedance of high- T_c superconductor samples," *Solid State Commun.*, vol. 78, no. 7, pp. 631–633, May 1991.

[2] C. Wilker, Z.-Y. Shen, V. X. Nguyen, and M. S. Brenner, "A sapphire resonator for microwave characterization of superconducting thin films," in *Proc. Appl. Supercond. Conf.*, Chicago, IL, Aug. 24–28, 1992, pp. 38–47.

[3] J. Krupka, M. Klinger, M. Kuhn, A. Baranyak, M. Stiller, J. Hinken, and J. Modelski, "Surface resistance measurements of HTS films by means of sapphire dielectric resonators," *IEEE Trans. Appl. Supercond.*, vol. 3, no. 3, pp. 3043–3048, Sep. 1993.

[4] [Online]. Available: http://www.theva.com/prod

[5] S. Sridhar and W. L. Kennedy, "Novel technique to measure the microwave response of high Tc superconductors between 4.2 and 200 K," *Rev. Sci. Instrum.*, vol. 59, no. 4, pp. 531–536, Apr. 1988.

[6] L. Dietl and U. Trinks, "The surface-resistance of a superconducting lead tin alloy," *Nucl. Instrum. Methods Phys. A*, vol. 284, no. 2/3, pp. 293–295, Dec. 1989.

[7] D. A. Bonn, D. C. Morgan, and W. N. Hardy, "Split-ring resonators for measuring microwave surface resistance of oxide superconductors," *Rev. Sci. Instrum.*, vol. 62, no. 7, pp. 1819–1823, Jul. 1991.

[8] N. Pompeo, L. Muzzi, V. Galluzzi, R. Marcon, and E. Silva, "Measurements and removal of substrate effects on the microwave surface impedance of YBCO films on $SrTiO_3$," *Supercond. Sci. Technol.*, vol. 20, no. 10, pp. 1002–1008, Oct. 2007.

[9] S. Sridhar, "Microwave response of thin film superconductors," *J. Appl. Phys.*, vol. 63, no. 1, pp. 159–166, Jan. 1988.

[10] N. Klein, H. Chaloupka, G. Muller, S. Orbach, H. Piel, B. Roas, L. Schultz, U. Klein, and M. Peiniger, "The effective microwave surface impedance of high Tc thin films," *J. Appl. Phys.*, vol. 67, no. 11, pp. 6940–6945, Jun. 1990.

[11] P. L. Bender and C. J. Gorter, "A few remarks on the two-fluid model for superconductors," *Physica*, vol. 18, no. 8/9, pp. 597–604, Aug./Sep. 1952.

[12] M. Tinkham, *Introduction to Superconductivity*. New York: McGraw-Hill, 1996, ch. 2.

[13] J. Krupka and W. Strupinski, "Measurements of the sheet resistance and conductivity of thin epitaxial graphene and SiC films," *Appl. Phys. Lett.*, vol. 96, no. 8, pp. 082101-1–082101-3, Feb. 2010.

[14] S. Maj and M. Pospieszalski, "A composite multilayered cylindrical dielectric resonator," in *IEEE MTT-S Dig.*, San Francisco, CA, May 30–Jun. 1, 1984, pp. 190–191.

[15] J. Krupka, K. Derzakowski, A. Abramowicz, J. Ceremuga, and R. G. Geyer, "Application of mode matching technique for modeling of cylindrical dielectric resonators containing multilateral superconducting, metal and dielectric media," in *Proc. NUMELEC Conf.*, Lyon, France, Mar. 19–21, 1997.

[16] J. Krupka, K. Derzakowski, T. Zychowicz, B. L. Givot, W. C. Egbert, and M. M. David, "Measurements of the surface resistance and conductivity of thin conductive films at frequency about 1 GHz employing dielectric resonator technique," *J. Eur. Ceram. Soc.*, vol. 27, no. 8/9, pp. 2823–2826, 2007.

[17] G. Muller, N. Klein, A. Brust, H. Chaloupka, M. Hein, S. Orbach, H. Piel, and D. Reschke, "Survey of microwave surface impedance data of high-Tc superconductors—Evidence for nonpairing charge carriers," *J. Supercond.*, vol. 3, no. 3, pp. 235–242, Sep. 1990.

J. Krupka, biography not available at the time of publication.

J. Wosik, biography not available at the time of publication.

C. Jastrzębski, biography not available at the time of publication.

T. Ciuk, biography not available at the time of publication.

J. Mazierska, biography not available at the time of publication.

M. Zdrojek, biography not available at the time of publication.